3-1970

High-Temperature Expansion for the Orientational Specific Heat of Solid H_2 and D_2

A. John Berlinsky

A. Brooks Harris
University of Pennsylvania, harris@sas.upenn.edu

Recommended Citation

Berlinsky, A., & Harris, A. (1970). High-Temperature Expansion for the Orientational Specific Heat of Solid H_2 and D_2. *Physical Review A, 1* (3), 878-887. http://dx.doi.org/10.1103/PhysRevA.1.878

High-Temperature Expansion for the Orientational Specific Heat of Solid H_2 and D_2

Abstract

Terms up to order $(\Gamma/k_BT)^5$ in the high-temperature expansion of the orientational specific heat of ortho-para alloys of solid H_2 or D_2 are evaluated. Good agreement is obtained between theory and experiment using a Padé approximant and effective values of the quadrupolar coupling constant, $\Gamma_{eff}/\Gamma_0=0.83$ for D_2 and $\Gamma_{eff}/\Gamma_0=0.80$ for H_2, where Γ_0 is the value for a rigid lattice. These values agree with other determinations of Γ_{eff}, whereas the T^{-2} approximation for the specific heat yields anomalously small values of Γ_{eff}.

Disciplines

Physics

High-Temperature Expansion for the Orientational Specific Heat of Solid H_2 and D_2†

A. John Berlinsky and A. Brooks Harris*
Department of Physics, University of Pennsylvania, Philadelphia, Pennsylvania 19104
(Received 19 September 1969)

Terms up to order $(\Gamma/k_BT)^5$ in the high-temperature expansion of the orientational specific heat of ortho-para alloys of solid H_2 or D_2 are evaluated. Good agreement is obtained between theory and experiment using a Padé approximant and effective values of the quadrupolar coupling constant, $\Gamma_{\rm eff}/\Gamma_0 = 0.83$ for D_2 and $\Gamma_{\rm eff}/\Gamma_0 = 0.80$ for H_2, where Γ_0 is the value for a rigid lattice. These values agree with other determinations of $\Gamma_{\rm eff}$, whereas the T^{-2} approximation for the specific heat yields anomalously small values of $\Gamma_{\rm eff}$.

I. INTRODUCTION

The interactions between molecules in solid hydrogen[1] have been a subject of widespread interest recently. Nakamura[2] was the first to establish the general nature of these interactions as arising from the electric quadrupole-quadrupole (EQQ) interactions between molecules. He also attempted to explain quantitatively the orientational specific heat[3] of solid H_2 at temperatures above 4 K in terms of an estimate of the EQQ coupling parameter Γ. More recently, Grenier and White[4] have carried out a similar analysis of their specific-heat data for solid D_2 at high ($T > 6$ K) temperatures. In both cases the specific heat was fitted to a T^{-2} law corresponding to the effective values $\Gamma_{\rm eff} = 0.52$ cm^{-1} and $\Gamma_{\rm eff} = 0.41$ cm^{-1} for D_2 and H_2, respectively.

However, these values of the EQQ coupling constant are much smaller than one would expect. According to the most recent theoretical calculations,[5,6] the quadrupole moments of the H_2 and D_2 molecules are[5] $Q = 0.4883 a_0^2$ and $Q = 0.4783 a_0^2$, respectively, where a_0 is the Bohr radius. These values of Q, together with the observed lattice constant[7-9] R, enable one to calculate the EQQ interaction constant[10] $\Gamma_0 = 6e^2Q^2/25R^5$ as $\Gamma_0 = 0.839$ cm^{-1} for D_2 and $\Gamma_0 = 0.698$ cm^{-1} for H_2. The discrepancy between these values and those obtained experimentally is rather serious in that to remove the discrepancy would require attributing more than a 100% error to the observed orientational specific heat. The object of the present work was to study further terms in the high-temperature expansion of the specific heat to see if they could provide an explanation for this anomaly in the specific-heat data.

Before describing the calculations, we should point out that one can expect departures from the rigid lattice values of Γ_0 quoted above. Such departures have been calculated[11,12] as arising from (i) dielectric screening, (ii) static phonon renormalization, and (iii) dynamic phonon renormalization. The physical picture of these mechanisms is discussed fully in Refs. 11 and 12. The results of such calculations show that at high temperatures, i.e., for $k_BT \gg \Gamma_0$, Γ_0 should be replaced by $\Gamma_{\rm eff}$, with $\Gamma_{\rm eff}/\Gamma_0 \approx 0.88$ for both H_2 and D_2. Even using these reduced values of $\Gamma_{\rm eff}$ one finds a specific heat in the T^{-2} approximation about twice as large as that actually observed. As our analysis will show, this discrepancy is simply the result of not keeping enough terms in the high-temperature expansion for the specific heat.

This paper is organized as follows: In Sec. II, we outline the diagrammatic formalism needed for a calculation of the high-temperature specific-heat series. In Sec. III, we give detailed numerical results for each diagram introduced in the calculation. In Sec. IV, we compare the various forms of our results with the experimental data. We find that quite reasonable agreement between theory and experiment is obtained with a Padé approximant, using the values $\Gamma_{\rm eff} = 0.70$ cm^{-1} $= 0.83\ \Gamma_0$ for D_2, and $\Gamma_{\rm eff} = 0.56$ cm^{-1} $= 0.80\ \Gamma_0$ for H_2. These values are comparable with those predicted, taking account of the renormalizations discussed above. Furthermore, from the behavior of the first four terms in the high-temperature expansion, we infer that high-temperature behavior does not obtain below about $k_BT/\Gamma = 10$ for, say, 50% concentration of molecules with $J = 1$. This finding probably explains why the two-term high-temperature expansion used to analyze the second moment of the NMR spectrum of solid H_2[13-14] in the temperature range 4 K $< T <$ 10 K is only qualitatively successful.[15]

II. FORMALISM

Since the EQQ interactions are dominant,[2] it is reasonable to describe the molecular rotations in solid hydrogen by the following simple model Hamiltonian:

$$\mathcal{H} = \mathcal{H}_{KE} + \mathcal{H}_{EQQ} , \tag{1}$$

where the first term is the Hamiltonian for the rotational kinetic energy,

$$\mathcal{H}_{KE} = B \sum_i J_i (J_i + 1) , \tag{2a}$$

and the second is the EQQ Hamiltonian, for which we use the convenient form given by Gush and Van Kranendonk,[16]

$$\mathcal{H}_{EQQ} = \tfrac{20}{9}\pi (70\pi)^{1/2} \sum_{(i,j)} \sum_{m,n} C(224; mn) \times Y_2^{\,m}(\Omega_i) Y_2^{\,n}(\Omega_j) Y_4^{\,m+n}(\Omega_{ij})^* . \tag{2b}$$

Here, J_i is the angular momentum of the ith molecule associated with molecular rotation; the $Y_L^{\,m}$ are spherical harmonics in the phase convention of Rose[17]; $\Omega_i \equiv (\theta_i, \varphi_i)$ and $\Omega_j \equiv (\theta_j, \varphi_j)$ specify the orientation of the symmetry axes of the ith and jth molecules, respectively, with respect to some external coordinate system; $\Omega_{ij} \equiv (\theta_{ij}, \varphi_{ij})$ specifies the orientation of the line joining the ith and jth molecules with respect to this same coordinate system; and $C(224; m,n)$ is a Clebsch-Gordan coefficient.[17] In Eq. (2b), (i,j) indicates that the sum is over pairs, with i and j nearest neighbors. The lattice structure of solid hydrogen in the temperature range of interest is hexagonal close-packed (hcp). Note that $B \gg \Gamma$, which justifies our treating J as a good quantum number. Furthermore, since transitions between even and odd parity states are strongly forbidden, at low temperatures the solid will be an alloy consisting of a fraction x of $(J=1)$ molecules and a fraction $(1-x)$ of $(J=0)$ molecules. It is obvious that within our approximations the interactions are nonvanishing only between pairs of $(J=1)$ molecules. In writing Eq. (2b), we have neglected interactions between other than nearest neighbors, For terms in the specific heat of order x^2, direct calculations show that this approximation introduces errors of the order of 1%. For terms of higher order in x, such calculations are extremely cumbersome and have not been undertaken. However, it would be surprising if the effects of further neighbor interactions were more important here than in the calculation of the molecular field, where they lead to an 11% correction.[18,19]

We begin the calculation by developing a general expression for the specific heat, closely following the treatment of Horowitz and Callen.[20] To do this we note that $\mathcal{H}_{EQQ}$ is a sum of pairwise interactions

$$\mathcal{H}_{EQQ} = \sum_{(i,j)} H_{ij} , \tag{3}$$

and that H_{ij} commutes with the H_{kl}, unless i or j is equal to k or l. We now consider the free energy F, which we write as

$$-\beta F = \ln \left\langle e^{-\beta \mathcal{H}_{EQQ}} \right\rangle , \tag{4}$$

where, for any operator θ, $\langle\theta\rangle$ denotes $\mathrm{Tr}\theta/\mathrm{Tr}I$, where I is the unit operator. We wish to write the free energy as a power series of the form

$$-\beta F = \sum_{n=1}^{\infty} \beta^n (n!)^{-1} M_n(\mathcal{H}_{EQQ}) . \tag{5}$$

Following Ref. 20, it is convenient to introduce the definitions

$$\rho_{\{\alpha\}} = \rho_0 \exp\left(\sum_{(i,j)} H_{ij} \alpha_{ij} \right), \qquad \rho_0 = (\mathrm{Tr}I)^{-1}, \tag{6}$$

$$\langle \mathcal{H}_{EQQ} \rangle_{\{\alpha\}} = \mathrm{Tr}(\rho_{\{\alpha\}} \mathcal{H}_{EQQ}) / \mathrm{Tr}\rho_{\{\alpha\}} , \tag{7}$$

$$D_{\{\alpha\}} = \sum_{(i,j)} \frac{\partial}{\partial \alpha_{ij}} = \sum_{(i,j)} D_{ij} . \tag{8}$$

Then we can write

$$-\beta F = \lim_{\{\alpha\} \to 0} \ln \mathrm{Tr} \left(e^{-\beta \mathcal{H}_{EQQ}} \rho_{\{\alpha\}} \right) , \tag{9a}$$

$$-\beta F = \lim_{\{\alpha\} \to 0} \ln \mathrm{Tr} \left[\exp\left(\sum_{(i,j)} (\alpha_{ij} - \beta) \mathcal{H}_{ij} \right) \right] , \tag{9b}$$

$$-\beta F = \lim_{\{\alpha\} \to 0} \exp(-\beta D_{\{\alpha\}}) \times \ln \mathrm{Tr} \left[\exp\left(\sum_{(i,j)} \alpha_{ij} H_{ij} \right) \right] , \tag{9c}$$

where the operator $e^{-\beta D_{\{\alpha\}}}$ is a translation operator of several variables which transforms a function of α_{ij} into a function of $\alpha_{ij} - \beta$ for all pairs (i,j). Now we simply expand $e^{-\beta D_{\{\alpha\}}}$ as a power series in β and we find

$$-\beta F = \lim_{\{\alpha\} \to 0} \sum_{n=1}^{\infty} (n!)^{-1} \times \left(-\beta \sum_{(i,j)} D_{ij} \right)^n \ln \mathrm{Tr}\, \rho_{\{\alpha\}} . \tag{10}$$

Here we have taken note of the fact that the $(n=0)$ term is simply $(\ln 1) = 0$.

Thus, comparing this result with Eq. (5) we have the nth cumulant

$$M_n(\mathcal{H}_{\mathrm{EQQ}}) = \lim_{\{\alpha\}\to 0}\left(-\beta\sum_{(i,j)} D_{ij}\right)^n \times \ln \mathrm{Tr}\rho_{\{\alpha\}} \ . \tag{11}$$

We may expand the sum over (i,j) using the multinomial theorem

$$\left(-\beta\sum_{(i,j)} D_{ij}\right)^n = n! \sum_{\{p_{ij}\}} \prod_{(i,j)} \frac{(-\beta D_{ij})^{p_{ij}}}{p_{ij}!} \ , \tag{12a}$$

where $\sum_{(i,j)} p_{ij} = n$. Then if we define

$$M\{p_{ij}\} = \prod_{(i,j)} D_{ij}^{\,p_{ij}} \ln \mathrm{Tr}\rho_{\{\alpha\}} \ , \tag{12b}$$

we may rewrite the free energy as

$$-\beta F = \sum_{\{p_{ij}\}}\left(\prod_{(i,j)} \frac{(-\beta)^{p_{ij}}}{p_{ij}!}\right) M\{p_{ij}\} \ , \tag{13}$$

where the sum over n is performed by removing the restriction on the sum of the p_{ij}. This result is most easily understood in terms of a diagrammatic representation. Let each of the $M\{p_{ij}\}$ correspond to a diagram with p_{ij} links joining the ith and jth lattice sites. It is a well-known result that only connected diagrams will have a nonzero value.

The sum over p_{ij} can be converted into a sum over all possible connected diagrams. For our Hamiltonian the value of a diagram is strongly dependent on its shape; so we have to sum over all differently shaped diagrams, not merely over all topologically distinct ones. This process is considerably simplified by the fact that we are only considering nearest-neighbor interactions. Another simplification results from the fact that all diagrams which have a free end are equal to zero, because in this case the term will contain a factor $\mathrm{Tr}\,Y_2^{\,m}$, which is zero. For example, the lowest-order diagram is a single link between i and j:

$$M\{p_{kl}\} = \langle H_{ij}\rangle = 0 \ , \tag{14a}$$

$$\text{with} \quad p_{kl} = \delta_{ik}\delta_{jl} \ , \tag{14b}$$

where δ is the Kronecker delta. The lowest-order nonzero term is when $p_{kl} = 2\delta_{ik}\delta_{jl}$. For this case,

$$M\{p_{kl}\} = \langle H_{ij}^{\,2}\rangle - \langle H_{ij}\rangle^2 = \langle H_{ij}^{\,2}\rangle \ . \tag{15}$$

If the solid were 100% ($J=1$) molecules, this diagram would occur $6N$ times, where N is the total number of molecules, since the coordination number of the hcp lattice is $z=12$. However, when the concentration of ($J=1$) molecules is x, this diagram will occur $6Nx^2$ times, assuming a random alloy.[21] Thus, to lowest order

$$F = -3\beta x^2 N\langle H_{ij}^{\,2}\rangle \ . \tag{16}$$

Similarly, for each diagram the sum over $\{p_{ij}\}$ is replaced by the number of times the same shaped diagram occurs in the lattice multiplied by a factor x^s, where s is the number of lattice sites in the diagram.

Accordingly, our final expression for the free energy is

$$-\beta F = N \sum_{\substack{i=\text{all}\\ \text{diagrams}}} \beta^{n_i}(p_1^{(i)}!p_2^{(i)}!\cdots)^{-1} \times a_i x^{s_i} M\{p^{(i)}\} \ , \tag{17}$$

where Na_i is the number of times the ith diagram occurs in the lattice, n_i is the number of bonds in the diagram, and $p_1^{(i)}, p_2^{(i)}, \ldots$, etc., are the nonzero multiplicities of bonds 1, 2, ..., of the ith diagram. To obtain the specific heat, we use

$$C_V = -T\frac{\partial^2 F}{\partial T^2} \ , \tag{18}$$

which yields

$$\frac{C_V}{R} = \sum_{\substack{i=\text{all}\\ \text{diagrams}}} n_i(n_i-1) \times (p_1^{(i)}!p_2^{(i)}!\ldots)^{-1} a_i x^{s_i} D_i(-\beta\Gamma)^{n_i} \ , \tag{19}$$

$$\text{where} \quad D_i = M\{p^{(i)}\}/\Gamma^{n_i} \ . \tag{20}$$

III. RESULTS FOR DIAGRAMS

In this section, we will give explicit results for all diagrams required for the calculations of the terms in the specific heat up to order $(\beta\Gamma)^5$. The difficult part of these computations was the calculation of the D_i. In general, these involve multiple sums of products of Clebsch-Gordan coefficients and fourth-rank spherical harmonics. However, for the special case of two sites, i.e., $s_i = 2$, the value of D_i for arbitrary values of n_i can be computed very simply from the known[2] energy

levels of an isolated pair of ($J=1$) molecules. Nontrivial terms, i.e., those involving more than two sites, rapidly become more complicated as n_i increases. For the lowest-order nontrivial term ($n_i=3$), we verified the result given by Nakamura.[2] For the cases $n_i=4$ and 5, these summations were carried out numerically on an electronic computer. The results, along with the various combinatorial factors, are listed in Tables I and II. The diagrams are labeled $(n_i;p_1^{(i)},p_2^{(i)},\dots)$ with additional subscripts giving shape parameters and, where necessary, superscripts T, Q, and P denoting triangle, quadrilateral, and pentagon, respectively, as is illustrated in Figs. 1 and 2. In Secs. B and C of Table II, we specify the shapes of the diagrams by giving spherical polar angles for each bond. These specifications are not unique, since the shape of the diagram is invariant under rigid rotations. The values are simply one possible set of arguments for the spherical harmonics which appear in the expressions for these diagrams. Finally, the complete coefficients of $x^m(\beta\Gamma)^n$ in the specific-heat expansion for $n\leq 5$ are given in Table III.

In an elaborate calculation such as this, it is essential to be able to check the validity of both the analytic expressions and their numerical evaluation by computer. The values of the various Na_i, the number of times each diagram occurs in the lattice, are fairly obvious for single bonds and triangles. For the somewhat more complicated cases of quadrilaterals and pentagons, we were able to compare our count of the sum of individual shapes to the results of Domb and Sykes[22] for the total number of quadrilaterals and pentagons in the hcp lattice. The values of the individual diagrams D_i, (except for the trivial ones) were checked for rotational invariance. That is, for each of the figures the computation was performed with at least two different sets of spherical angles specifying the shape. This is a very delicate test, not only of the programming, but also of the analytic expression, because in general even the introduction of spurious phase factors (-1) will destroy the rotational invariance. In addition, one of us[23] had calculated the eigenvalues for the EQQ interaction between three ($J=1$) molecules at the vertices of an equilateral triangle. From those results, we have

$$S_3\Gamma^3\equiv\tfrac{1}{27}\textstyle\sum_i\lambda_i^{\,3}=3\langle H_{ij}^{\,3}\rangle+6\langle H_{ij}H_{jk}H_{ki}\rangle=42.09\Gamma^3\,, \tag{21a}$$

$$S_4\Gamma^4\equiv\tfrac{1}{27}\textstyle\sum_i\lambda^4=3\langle H_{ij}^{\,4}\rangle+36\langle H_{ij}^{\,2}H_{jk}H_{ki}\rangle+18\langle H_{ij}^{\,2}H_{jk}^{\,2}\rangle=1386.4\Gamma^4\,, \tag{21b}$$

$$S_5\Gamma^5\equiv\tfrac{1}{27}\textstyle\sum_i\lambda_i^{\,5}=3\langle H_{ij}^{\,5}\rangle+60\langle H_{ij}^{\,3}H_{jk}H_{ki}\rangle+90\langle H_{ij}^{\,2}H_{jk}^{\,2}H_{ki}\rangle+60\langle H_{ij}^{\,2}H_{jk}^{\,3}\rangle=6664.8\Gamma^5\,, \tag{21c}$$

TABLE I. Factors for diagrams with less than five bonds.

Diagram [a]	s_i	a_i	$M\{p_i\}$	D_i
(2;2)	2	6	$\langle H_{ij}^{\,2}\rangle$	$\frac{70}{9}$
(3;3)	2	6	$\langle H_{ij}^{\,3}\rangle$	10
(3;1,1,1)	3	8	$\langle H_{ij}H_{jk}H_{ki}\rangle$	$\frac{3095}{1536}$
(4;4)	2	6	$\langle H_{ij}^{\,4}\rangle-3\langle H_{ij}^{\,2}\rangle^2$	$\frac{530}{27}$
(4;2,1,1)	3	24	$\langle H_{ij}^{\,2}H_{jk}H_{ki}\rangle$	$\frac{18\,545}{13\,824}$
$(4;2,2)_\theta$				
$\theta=\frac{1}{3}$		24	$\langle H_{ij}^{\,2}H_{jk}^{\,2}\rangle$	−19.663
$\theta=\frac{2}{3}$		18		−19.663
$\theta=\frac{1}{2}$	3	12	$-\langle H_{ij}^{\,2}\rangle\langle H_{jk}^{\,2}\rangle$	−22.022
$\theta=1$		3		−7.901
$\theta=1-2b$		3		−21.070
$\theta=c$		6		−13.542
(4;1,1,1,1)				
$\theta=\frac{1}{3}$ $\varphi=1$		9		−1.923
$\theta=\frac{1}{2}$ $\varphi=1$		3		6.778
$\theta=\frac{1}{3}$ $\varphi=2b$	4	6	$\langle H_{ij}H_{jk}H_{kl}H_{li}\rangle$	0.782
$\theta=\frac{1}{3}$ $\varphi=4b$		3		−1.812
$\theta=\frac{1}{3}$ $\varphi=1-2b$		12		−0.666

[a] All angles are quoted in multiples of π, $b=\pi^{-1}\arctan(\frac{1}{2}\sqrt{2})$, and $c=\pi^{-1}\arccos(-\frac{5}{6})$.

TABLE II. Part (A): Factors for diagrams with five bonds. [a] Part (B): Factors for $(5;2,1,1,1)^{Q_2}$. Part (C): Factors for pentagons, $(5;1,1,1,1,1)^{P}$.

(A)

Diagram	s_i	a_i	$M\{p_i\}$	D_i
$(5;5)$	2	6	$\langle H_{ij}{}^5\rangle - 10\langle H_{ij}{}^2\rangle\langle H_{ij}{}^3\rangle$	$-\frac{1270}{9}$
$(5;3,1,1)$	3	24	$\langle H_{ij}{}^3 H_{jk}H_{ki}\rangle - 3\langle H_{ij}{}^2\rangle\langle H_{jk}H_{ki}H_{ij}\rangle$	-21.660
$(5;2,2,1)^T$	3	24	$\langle H_{ij}{}^2 H_{jk}{}^2 H_{ki}\rangle$	11.178
$(5;3,2)_\theta$				
$\theta=\frac{1}{3}$		48		-40.65
$\theta=\frac{2}{3}$		36		-40.65
$\theta=\frac{1}{2}$	3	24	$\langle H_{ij}{}^3 H_{jk}{}^2\rangle$	-51.76
$\theta=1$		6	$-\langle H_{ij}{}^3\rangle\langle H_{jk}{}^2\rangle$	5.185
$\theta=1-2b$		6		-47.08
$\theta=c$		12		-15.75
$(5;2,1,1,1)_{\theta,\varphi}{}^{Q_1}$				
$\theta=\frac{1}{3}\quad\varphi=1$		36		-4.880
$\theta=\frac{1}{2}\quad\varphi=1$		12	$\langle H_{ij}{}^2 H_{jk}H_{kl}H_{li}\rangle$	11.616
$\theta=\frac{1}{3}\quad\varphi=2b$	4	24		0.221
$\theta=\frac{1}{3}\quad\varphi=4b$		12		-1.767
$\theta=\frac{1}{3}\quad\varphi=1-2b$		48		-1.254
$(5;1,1,1,1,1)_{\theta,\varphi}{}^{Q}$				
$\theta=\frac{1}{3}\quad\varphi=1$		9		-4.092
$\theta=\frac{1}{3}\quad\varphi=2b$	4	12	$\langle H_{ij}H_{jk}H_{ki}H_{kl}H_{li}\rangle$	0.118
$\theta=\frac{1}{3}\quad\varphi=4b$		3		-2.910
$\theta=\frac{1}{3}\quad\varphi=1-2b$		12		1.477
$(5;2,2,1)^Q$	4	6 [b]	$\langle H_{ij}{}^2 H_{jk}H_{kl}{}^2\rangle$	-26.04 [b]

(B) [c]

$s_i=4 \quad M\{p_i\}=\langle H_{ij}{}^2 H_{ik}H_{kl}H_{li}\rangle - \langle H_{ij}{}^2\rangle\langle H_{ik}H_{kl}H_{li}\rangle$

$\theta_{ik}=\frac{1}{2},\quad \varphi_{ik}=\frac{5}{3};\quad \theta_{kl}=\frac{1}{2},\quad \varphi_{kl}=1;\quad \theta_{li}=\frac{1}{2},\quad \varphi_{li}=\frac{1}{3}$

θ_{ij}	φ_{ij}	a_i	D_i
$\frac{1}{2}$	$\frac{1}{3}$	12	2.9990
$\frac{1}{2}$	0	12	-8.8689
b	$\frac{7}{6}$	12	-0.3617
b	$\frac{1}{2}$	12	3.5943
b	$\frac{11}{6}$	12	-0.3617

$\theta_{ik}=\frac{1}{2},\quad \varphi_{ik}=1;\quad \theta_{kl}=1-b,\quad \varphi_{kl}=\frac{1}{6};\quad \theta_{li}=b,\quad \varphi_{li}=\frac{11}{6}$

θ_{ij}	φ_{ij}	a_i	D_i
$\frac{1}{2}$	$\frac{2}{3}$	12	3.5943
$\frac{1}{2}$	$\frac{1}{3}$	12	-0.3617
$\frac{1}{2}$	0	12	2.9990
$\frac{1}{2}$	$\frac{5}{3}$	12	3.5943
$\frac{1}{2}$	$\frac{4}{3}$	12	-0.3617
b	$\frac{5}{6}$	12	-5.5275
b	$\frac{1}{6}$	12	3.7031
b	$\frac{3}{2}$	12	-4.4072
$1-b$	$\frac{1}{6}$	12	-8.8689
$1-b$	$\frac{3}{2}$	12	-0.3617

TABLE II. (*continued*).

$\theta_{ik}=b$, $\varphi_{ik}=\frac{11}{6}$; $\theta_{kl}=\frac{1}{2}$, $\varphi_{kl}=1$; $\theta_{li}=1-b$, $\varphi_{li}=\frac{1}{6}$

θ_{ij}	φ_{ij}	a_i	D_i
$\frac{1}{2}$	$\frac{1}{3}$	12	−0.3617
$\frac{1}{2}$	0	12	−8.8689
$\frac{1}{2}$	$\frac{5}{3}$	12	−0.3617
b	$\frac{1}{2}$	6	3.5943
$1-b$	$\frac{7}{6}$	6	1.5054
$1-b$	$\frac{1}{2}$	6	6.5816
$1-b$	$\frac{11}{6}$	6	1.5054

(C)[d]

$s=5$ $M\{p_i\}=\langle H_{ij}H_{jk}H_{kl}H_{lm}H_{mi}\rangle$

(θ_1,φ_1)	(θ_2,φ_2)	(θ_3,φ_3)	(θ_4,φ_4)	(θ_5,φ_5)	a_i	D_i
$(\frac{1}{2},0)$	$(\frac{1}{2},\frac{2}{3})$	$(\frac{1}{2},1)$	$(\frac{1}{2},\frac{4}{3})$	$(\frac{1}{2},0)$	12	1.4771
$(b,\frac{1}{6})$	$(1-b,\frac{1}{2})$	$(1-b,\frac{5}{6})$	$(\frac{1}{2},\frac{4}{3})$	$(b,\frac{11}{6})$	6	−0.3900
$(\frac{1}{2},\frac{2}{3})$	$(\frac{1}{2},\frac{4}{3})$	$(1-b,\frac{3}{2})$	$(\frac{1}{2},0)$	$(b,\frac{1}{2})$	18	2.8103
$(\frac{1}{2},\frac{2}{3})$	$(\frac{1}{2},\frac{4}{3})$	$(b,\frac{1}{2})$	$(\frac{1}{2},0)$	$(1-b,\frac{3}{2})$	24	2.8103
$(\frac{1}{2},\frac{1}{3})$	$(\frac{1}{2},\frac{2}{3})$	$(b,\frac{3}{2})$	$(1-b,\frac{7}{6})$	$(\frac{1}{2},\frac{5}{3})$	36	−1.4775
$(\frac{1}{2},0)$	$(b,\frac{1}{6})$	$(b,\frac{7}{6})$	$(1-b,\frac{5}{6})$	$(1-b,\frac{7}{6})$	12	−0.5543
$(\frac{1}{2},\frac{2}{3})$	$(b,\frac{2}{3})$	$(1-b,\frac{7}{6})$	$(1-b,\frac{1}{6})$	$(b,\frac{11}{6})$	6	−3.4845
$(b,\frac{1}{2})$	$(b,\frac{3}{2})$	$(\frac{1}{2},0)$	$(1-b,\frac{7}{6})$	$(1-b,\frac{5}{6})$	12	1.5822
$(\frac{1}{2},\frac{1}{3})$	$(\frac{1}{2},\frac{2}{3})$	$(b,\frac{7}{6})$	$(1-b,\frac{3}{2})$	$(\frac{1}{2},\frac{5}{3})$	36	−1.4775
$(b,\frac{1}{2})$	$(b,\frac{5}{6})$	$(1-b,\frac{7}{6})$	$(\frac{1}{2},\frac{5}{3})$	$(1-b,\frac{1}{6})$	6	2.6395

[a]All angles are quoted in multiples of π, and b and c are as in Table I.

[b]For this type of diagram, D_i is the sum over all orientations of the two end bonds keeping the central bond fixed. Thus, $a_i=6$ for this collection of diagrams.

[c]In this section, θ_{mn} and φ_{mn} are the polar and azimuthal angles, with respect to the crystal axis, of the bond corresponding to H_{mn}.

[d]In this section, θ_i and φ_i are the polar and azimuthal angles with respect to the crystal axes of succeeding bonds in the pentagons.

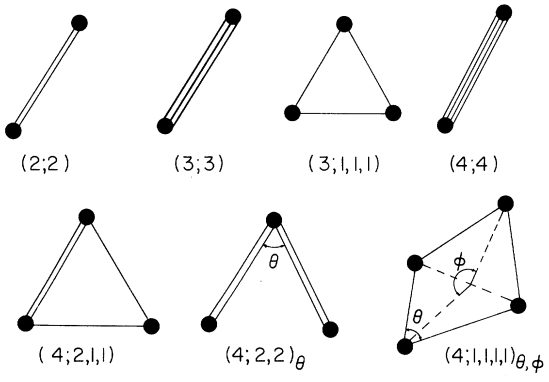

FIG. 1. Diagrams which contribute to terms up to order $(\beta\Gamma)^4$ in the orientational specific heat. For the quadrilateral, θ is the vertex angle, and φ is the dihedral angle as shown. The parameters are of the form $(n_1; p_1^{(i)}, p_2^{(i)}, \ldots)$.

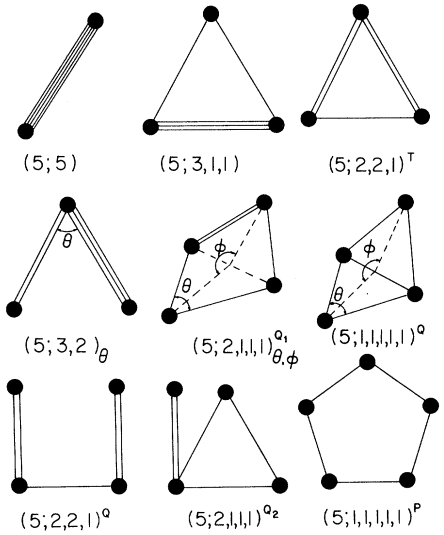

FIG. 2. Diagrams which contribute to the $(\beta\Gamma)^5$ term in the specific heat. For the quadrilaterals, the angles θ and φ are as in Fig. 1.

TABLE III. A_{mn} in $C/R = \sum_{mn} A_{mn} x^m (\Gamma\beta)^n$.

m^n	2	3	4	5
2	$\frac{140}{3}$	-60	$\frac{530}{9}$	$\frac{1270}{9}$
3		$-\frac{3095}{32}$	-3581.7	8886.7
4			-68.51	3872.9
5				-686.15

as compared to the corresponding values obtained using our numerical results for the D_i,

$$S_3 = 42.09 \ , \tag{22a}$$

$$S_4 = 1386.5 \ , \tag{22b}$$

$$S_5 = 6665.2 \ . \tag{22c}$$

This comparison served as a check on the values of all the triangular diagrams.

IV. COMPARISON WITH EXPERIMENT

Experimental determination of the orientational specific heat of solid hydrogen requires that two measurements be made of the total specific heat, one at the concentration of interest and the other at $x \approx 0$. If we make the reasonable assumption that the lattice specific heat is relatively insensitive to the concentration of $(J=1)$ molecules, then the orientational specific heat will be the difference of the two measurements.

A. D_2

For the case of $x \approx 0$, we use the measurements of Hill and Lounasmaa[24] on D_2 with $x = 0.015$. For the values of x of interest, we use the measurements of Grenier and White,[4] who have studied the specific heat of solid D_2 from $x = 0.331$ to 0.872. The experimental data was plotted versus temperature, and curves were drawn through the points. The curve for $x \approx 0$ gave the lattice specific heat which was subtracted from each of the other curves to give the orientational specific heat as a function of temperature at each of the various concentrations. The values so obtained agreed quite well with the graphical presentation of the orientational specific heat given in Ref. 4.

Error flags were drawn for the experimental points under the assumption that the probable error in each of the specific-heat measurements was about 3%. Since at high temperatures the relatively small rotational specific heat results from subtracting two large numbers, it is expected that its probable error will be considerably larger than 3%. This will be more noticeable at higher temperatures, where the lattice specific heat is larger and the rotational specific heat smaller. As the temperature increases still further, the experimental points become meaningless.

The experimental measurements which we use are not in fact measurements of C_V, the specific heat at constant volume, but rather they are measurements of C_S, the specific heat at saturated vapor pressure. We examined the difference $C_V - C_S$ for the experimental conditions and found it to be negligible compared to C_V below 10 K and unimportant compared to the large experimental error in the orientational specific heat in the region above 10 K.

When the power-series expansion of the specific heat, using the coefficients of Table III and taking $\Gamma_{\text{eff}} = 0.70\ \text{cm}^{-1} = 0.83\Gamma_0$, is plotted along with the experimental points, it is found that there is a strong divergence from the experimental values below about 10 K. This may be seen in Fig. 3, where the power series for $x = 0.594$ is labeled "4 term." In the same figure there are two curves labeled "[2,1] Padé" and "[1,2] Padé." These curves are two Padé approximants[25] to the above four-term expansion. For instance, the [2,1] Padé approximant has the form

$$C/R = A_{22}(x\beta\Gamma)^2 \frac{1 + B_1\beta\Gamma}{1 + C_1\beta\Gamma + C_2(\beta\Gamma)^2} \ , \tag{23}$$

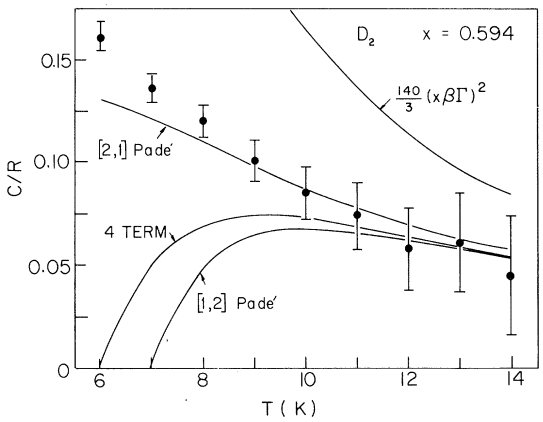

FIG. 3. Orientational specific heat of D_2 at high temperatures for $x = 0.594$. The experimental points are shown with their estimated errors. The curves labeled Padé are the [1,2] Padé approximant (below) and the [2,1] Padé approximant (above). Also shown are curves for the specific heat as obtained (i) by keeping only the leading term of order $(\beta\Gamma)^2$ in Eq. (19) and (ii) by keeping the first four terms in Eq. (19), i.e., those of order at most $(\beta\Gamma)^5$. In all cases the value $\Gamma_{\text{eff}} = 0.70\ \text{cm}^{-1} = 0.83\Gamma_0$ was used.

where the coefficients B_1, C_1, and C_2 are, of course, functions of x. They are evaluated by expanding the Padé approximant in a power series and comparing it to the four-term expansion. We see from Fig. 3 that use of the [1,2] Padé gives a poorer fit to the data than the four-term expansion and hence this Padé approximant will not be used further. On the other hand, use of the [2,1] Padé approximant provides an expression which approximates the experimental data over a more extended temperature range. However, from Figs. 3–5 we see that even the [2,1] Padé approximant begins to diverge from the experimental curve below, say, $T=8$ K, i.e., for $k_BT/\Gamma=8$. Such behavior is to be expected in view of the fact that this model has a phase transition,[18] or at least almost a transition,[26] for $k_BT_c/\Gamma\approx 6,131$. Thus, eventually the ratio of successive terms in the specific-heat series must be at least as big as T_c/T. On the other hand, the experimental data is unreliable above 12 K, where the probable error becomes very large. Thus, the region in which we can expect good agreement is rather limited.

The other curve in Fig. 3 is the T^{-2} term in the specific-heat expansion, again with $\Gamma_{\rm eff}=0.70$ cm^{-1} $=0.83\Gamma_0$. It is clear from this figure that the T^{-2} term does not describe the data at all for $T<14$ K. Using the "bare" values of Γ_0 instead of $\Gamma_{\rm eff}$ would make the discrepancy considerably larger. In order to obtain a fit using only the T^{-2} term, it would be necessary to take $\Gamma_{\rm eff}=0.56$ cm$^{-1}=0.61\Gamma_0$. This value falls well outside the range of values of $\Gamma_{\rm eff}/\Gamma_0$ from other experiments,[27] such as the Raman spectroscopy[28] or $(\partial p/\partial T)_V$ measurements[29,30] which give $\Gamma_{\rm eff}/\Gamma_0\approx 0.81$ for concentrated ($J=1$) D_2 in the fcc phase, and $\Gamma_{\rm eff}/\Gamma_0\approx 0.88$ for the dilute ($J=1$) solid.

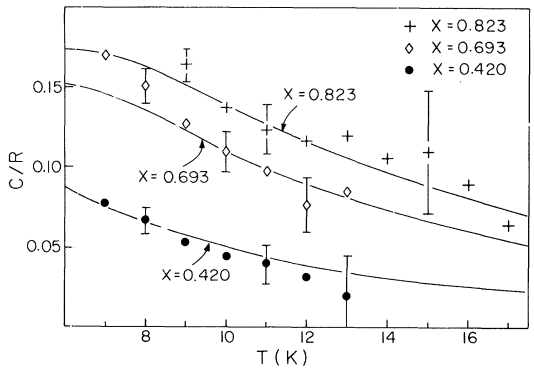

FIG. 4. Orientational specific heat of D_2 at high temperatures for three concentrations of ($J=1$) molecules. The solid curves are the [2,1] Padé approximants for the concentrations indicated, with $\Gamma_{\rm eff}=0.70$ cm$^{-1}=0.83\Gamma_0$.

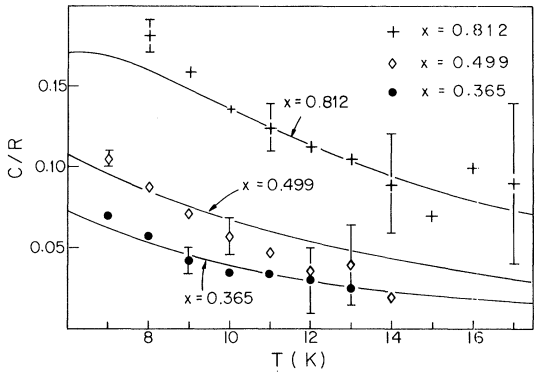

FIG. 5. Orientational specific heat of D_2 at high temperatures for three concentrations of ($J=1$) molecules. The solid curves are the [2,1] Padé approximants for the concentrations indicated, with $\Gamma_{\rm eff}=0.70$ cm^{-1} $=0.83\Gamma_0$.

Furthermore, we note that merely keeping terms up to order $(\beta\Gamma)^4$ also gives a very bad fit to the data because of the large negative coefficient A_{34}. The situation improves with the inclusion of the fifth-order terms, but it is only the Padé approximant which gives reasonable quantitative agreement. From Figs. 3–5, we see that this agreement is consistent for the various concentrations and is certainly within the experimental error of the data.

B. H_2

For the case of $x\approx 0$, we used the measurements of Hill and Lounasmaa[24] on solid H_2 with $x=2\times10^{-4}$. For the x values of interest, we obtained the specific heat from the graphical presentation of Hill and Ricketson,[3] who made measurements at $x=0.25$, $x=0.41$, $x=0.56$, and $x=0.74$. Considering the uncertainties in their method of determining the specific heat, it did not seem worthwhile to carry out an error analysis like that performed for D_2.

In Fig. 6, we compare the experimental values of the orientational specific heat with the theoretical values using the [2,1] Padé approximant. For this calculation we used the coefficients of Table III and took $\Gamma_{\rm eff}=0.56$ cm^{-1} which corresponds to $\Gamma_{\rm eff}/\Gamma_0=0.80$. As can be seen from the figure, although the fit is not as good as for D_2, it is still satisfactory in view of the experimental uncertainties. It should be mentioned that just as in the case of D_2 the T^{-2} approximation fails completely in the temperature range of interest unless one uses an extremely small value of $\Gamma_{\rm eff}$. Thus, with the same value of $\Gamma_{\rm eff}$ as for the Padé approximants one obtains for $x=0.56$ the dashed curve in Fig. 6 using the T^{-2} approximation. The value of $\Gamma_{\rm eff}$ we have used is quite comparable to the values obtained from other methods,[27] such as NMR,[13,15,31–35]

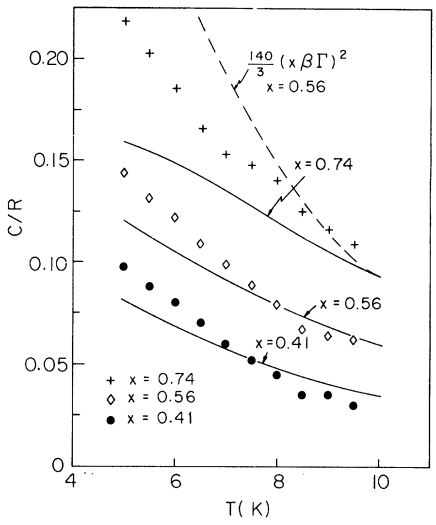

FIG. 6. Orientational specific heat of H_2 at high temperatures for three concentrations of ($J=1$) molecules. The solid curves are the [2, 1] Padé approximants for the concentrations indicated, with $\Gamma_{\text{eff}}=0.56\ \text{cm}^{-1}=0.80\Gamma_0$. The dashed curve is the T^{-2} approximation for the specific heat for $x=0.56$ using the same value of Γ_{eff}.

neutron scattering,[36,37] Raman spectroscopy,[28] or $(\partial p/\partial T)_V$ measurements.[38] These experiments give $\Gamma_{\text{eff}}/\Gamma_0 \approx 0.73$ for the concentrated ($J=1$) solid in the fcc phase, $\Gamma_{\text{eff}}/\Gamma_0 \approx 0.80$ for the dilute ($J=1$) solid, and from the only high-temperature determination, $\Gamma_{\text{eff}}/\Gamma_0 \approx 0.67$ from NMR data.

V. CONCLUSIONS

The conclusions which we may draw from our theoretical calculations and from a comparison of these with the experimental values are as follows. Firstly, the high-temperature expansion for the orientational specific heat converges very slowly even at, say, $k_BT/\Gamma=10$. Secondly, it is not possible to fit the specific-heat data with a T^{-2} expression using a reasonable value of Γ_{eff}. Thirdly, in the temperature range of interest it is found that a Padé approximant based on an expansion of the form $\sum A_{mn}x^m(\beta\Gamma)^n$ up to order $m=n=5$ fits the data rather well and gives a reasonable value of Γ_{eff}. Thus, we have attained a quantitative understanding of the orientational specific heat of solid hydrogen at high temperatures.

ACKNOWLEDGMENTS

The authors acknowledge helpful discussions with Professor H. Meyer and Professor D. White.

---

†Work supported in part by the National Science Foundation, under Grant No. GP 6771.

*Alfred P. Sloan postdoctoral Fellow, 1967–1969.

[1]The word hydrogen will be used to refer collectively to the isotopes H_2 and D_2.

[2]T. Nakamura, Progr. Theoret. Phys. (Kyoto) 14, 135 (1955).

[3]R. W. Hill and B. W. A. Ricketson, Phil. Mag. 45, 277 (1954).

[4]G. Grenier and D. White, J. Chem. Phys. 40, 3015 (1964).

[5]G. Karl and J. D. Poll, J. Chem. Phys. 46, 2944 (1967).

[6]L. Wolniewicz, J. Chem. Phys. 45, 515 (1966).

[7]W. H. Keesom, J. deSmedt, and H. H. Mooy, Commun. Kamerlingh Onnes Lab., Univ. Leiden 19, 209d (1930).

[8]R. L. Mills and A. F. Schuch, Phys. Rev. Letters 15, 722 (1965); A. F. Schuch and R. L. Mills, *ibid.* 16, 616 (1966).

[9]K. F. Mucker, S. Talhouk, P. M. Harris, and D. White, Phys. Rev. Letters 15, 586 (1965); K. F. Mucker, S. Talhouk, P. M. Harris, D. White, and R. A. Erickson, *ibid.* 16, 799 (1966); K. F. Mucker, P. M. Harris, D. White, and R. A. Erickson, J. Chem. Phys. 49, 1922 (1968).

[10]By Γ_0 we denote the bare EQQ interaction coefficient calculated ignoring any other interactions.

[11]A. B. Harris, Int. J. Quantum Chem. IIS, 347 (1968).

[12]A. B. Harris, Phys. Rev. (to be published).

[13]A. B. Harris and E. Hunt, Phys. Rev. Letters 16, 845 (1966); 16, 1233(E) (1966).

[14]L. I. Amstutz, H. Meyer, S. M. Myers, and D. C. Rorer, Phys. Rev. 181, 589 (1969).

[15]A. B. Harris (unpublished).

[16]H. P. Gush and J. Van Kranendonk, Can. J. Phys. 40, 1461 (1962).

[17]M. E. Rose, Elementary Theory of Angular Momentum (John Wiley & Sons, Inc., New York, 1957).

[18]H. M. James and J. C. Raich, Phys. Rev. 162, 649 (1967).

[19]J. Felsteiner, Phys. Rev. Letters 15, 1025 (1965).

[20]G. Horwitz and H. B. Callen, Phys. Rev. 124, 1757 (1961).

[21]This assumption is probably valid for D_2 and, at temperatures above 4 K, for H_2. In H_2 below this temperature, clustering effects become noticeable, see L. I. Amstutz, J. R. Thompson, and H. Meyer, Phys. Rev. Letters 21, 1175 (1968).

[22]C. Domb and M. F. Sykes, Phil. Mag. 2, 733 (1957).

[23]A. B. Harris (unpublished). The results are quoted by J. F. Jarvis, H. Meyer, and D. Ramm, Phys. Rev. 178, 1461 (1969). We would like to thank Dr. H. Miyagi for pointing out a misprint in one of the energy levels: for −3.620 read −3.630. The results then agree with those obtained by H. Miyagi, Progr. Theoret. Phys. (Kyoto) 40, 1448 (1968).

[24]R. W. Hill and O. V. Lounasmaa, Phil. Mag. 4, 785 (1959).

[25]G. A. Baker, Jr., Advan. Theor. Phys. 1, 1 (1965).
[26]A. B. Harris, Solid State Commun. 6, 149 (1968).
[27]A recent tabulation, including a reanalysis of some of the experimental determinations of Γ_{eff} is given by A. J. Berlinsky, A. B. Harris, and C. F. Coll, III, Solid State Commun. 7, 1491 (1969).
[28]W. N. Hardy, I. F. Silvera, and J. P. McTague, Phys. Rev. Letters 22, 297 (1969).
[29]D. Ramm, H. Meyer, J. F. Jarvis, and R. L. Mills, Solid State Commun. 6, 497 (1968).
[30]D. Ramm, H. Meyer, and R. L. Mills (to be published).
[31]A. B. Harris, L. I. Amstutz, H. Meyer, and S. M. Myers, Phys. Rev. 175, 603 (1968).
[32]M. Bloom, Physica 23, 767 (1957).
[33]W. P. A. Haas, G. Seidel, and N. J. Poulis, Physica 26, 834 (1960); W. P. A. Haas, N. J. Poulis, and J. J. W. Borleffs, *ibid.* 27, 1037 (1961).
[34]L. I. Amstutz, H. Meyer, S. M. Myers, and R. L. Mills, J. Phys. Chem. Solids 30, 2693 (1969).
[35]T. Moriya and K. Motizuki, Progr. Theoret. Phys. (Kyoto) 18, 183 (1957).
[36]W. Schott, H. Rietscel, and W. Glaser, Phys. Letters 27A, 566 (1968); W. Schott (private communications).
[37]R. J. Elliott and W. M. Hartmann, Proc. Phys. Soc. (London) 90, 671 (1967).
[38]J. F. Jarvis, H. Meyer, and D. Ramm, Phys. Rev. 178, 1461 (1969).

PHYSICAL REVIEW A VOLUME 1, NUMBER 3 MARCH 1970

Pressure and Electron Density Dependence of the Electron-Ion Recombination Coefficient in Helium

Jacques Berlande, Michel Cheret, Robert Deloche, Alain Gonfalone, and Claude Manus
Service de Physique Atomique Centre d'Etudes Nucléaires de Saclay, BP n° 2, Gif-sur-Yvette, 91, France
(Received 3 October 1969)

The dependence of the recombination coefficient α of He_2^+ ions and electrons on electron density and gas pressure is measured in helium afterglow plasmas where electron and gas temperatures are equal to 300 °K, gas pressure ranges from 10 to 100 Torr, and electron density from 10^9 to 5×10^{11} cm^{-3}. Electron density decay measured by microwave interferometry is compared with computer solutions of a continuity equation for electrons which takes into account ambipolar diffusion and recombination effects. One finds $\alpha=\alpha_2+k_e n_e+k_{\text{He}}n_{\text{He}}$, where n_e and n_{He} are the electron and neutral densities, respectively, and $\alpha_2\sim5\times10^{-10}$ cm^3 sec^{-1}, $k_e=(2\pm0.7)\times10^{-20}$ cm^6 sec^{-1}, $k_{\text{He}}=(2\pm0.5)\times10^{-27}$ cm^6 sec^{-1}. These values compare satisfactorily with results of theoretical computations for a collisional-radiative recombination mechanism including both collisions with electrons and neutrals. The effect of neutrals is particularly noteworthy as far as future experimental work on weakly ionized gases is concerned.

I. INTRODUCTION

A large amount of experimental work has been devoted to the study of electron-ion recombination processes in ionized helium.

When the gas pressure is low ($p\lesssim1$ Torr), it is recognized that the three-body process $He^+ + e + e \rightarrow He^* + e$ is the main recombination mechanism if the electron density is not too low or the electron temperature too high.

When the gas pressure is higher ($p\gtrsim5$ Torr) and He_2^+ is the dominant ion, the recombination process seems more complex. A summary of the work made before 1963 can be found in a paper by Oskam.[1] Most of the experimental results were presented or interpreted in terms of a two-body dissociative mechanism. It is suggested by Ferguson *et al.*[2] that a three-body process similar to that existing at low pressure $He_2^+ + e + e \rightarrow He_2^* + e$ could more satisfactorily explain recombination rates measured in helium afterglows, the dissociative mechanism being very improbable under the experimental conditions considered. Connor and Biondi,[3] the same year, referring to the conclusions of Ferguson *et al.*, pointed out that other processes must also be present to explain some of the experimental observations. Recently Born[4] found that for $p\sim10$–20 Torr, $n_e\sim10^{12}$–10^{13} cm^{-3}, and $T_e\sim1000$–2000 °K recombination is a three-body process involving two electrons.

Bates and Khare[5] made some estimates for helium of the recombination coefficient associated with a three-body neutral stabilized mechanism, $He^+ + e + He \rightarrow He^* + He$.[6] According to these authors, for a weakly ionized helium gas (i.e., for conditions often met in previous afterglow studies), the neutral stabilized mechanism may be competitive with the electron stabilized process. It is